Title
Correction to “Gate-Induced Intramolecular Charge Transfer in a Tunnel Junction: A Nonequilibrium Analysis”

Journal
The Journal of Physical Chemistry C, 117(35)

ISSN
1932-7447

Authors
Baratz, Adva
Galperin, Michael
Baer, Roi

Publication Date
2013-09-05

DOI
10.1021/jp4073476

Peer reviewed

Gate-induced intra-molecular charge-transfer in a tunnel junction: a non-equilibrium analysis

Adva Baratz[1], Michael Galperin[2*] and Roi Baer[1*]

[1]*Fritz Haber Center for Molecular Dynamics, Institute of Chemistry, the Hebrew University of Jerusalem, Jerusalem 91904 Israel.*

[2]*Department of Chemistry and Biochemistry, University of California at San Diego, La Jolla, CA 92093, USA.*

We study non-equilibrium effects in the conductance of a recently introduced molecular junction for which the gate acts as an on/off switch for an intra-junction electron-transfer between localized donor and acceptor sites. Using insights and parameters provided by DFT calculations, we build a double quantum-dot model that mimics the behavior of the molecular junction frontier orbitals. We employed the Redfield quantum master equation for calculating the steady-state populations, current and conductance channels; we show that the non-equilibrium population distribution has a significant effect on the conductance channels. While in some cases both equilibrium and non-equilibrium conductance channels coincide, in non-equilibrium additional channels appear.

Draft: Thursday, December 27, 2012

I. INTRODUCTION

In a recent paper,[1] two of us presented a molecular junction in which confinement and Coulomb effects are pronounced and controlled by well understood physical principles. A schematic depiction of the system is given in Figure 1, describing a Benzene-malononitrile (MN) acceptor displaced by a vertical distance $\bar{z}$ with respect to the trans-polyacetylene (PA) donor. The energy gap E_g for intramolecular electron transfer thus becomes dependent on the gate field E_z: $E_g(E_z) = I - A - e\bar{z}E_z$, where e is the electron charge and I and A are the ionization and affinity energies respectively (see caption of Figure 1). A sufficiently strong gate field will induce electron transfer from donor to acceptor, allowing sensitive control over the electronic properties of the junction. The gate effects on differential conductance channels have been studied extensively with respect to level alignment effects[2-16] when it controls electron transfer from a metal electrode to the molecule.[17-19] The present junction is unique in that the charge transfer is an intra-junction process and represents a reorganization of the electrons, leaving the junction largely uncharged.

Our previous analysis of this junction[1] was carried out using the generalized Kohn-Sham approach to density functional theory (DFT), employing a range-separated hybrid with first principles tuning of the range parameter, where the orbital energies have a meaning as quasiparticle energies.[20-22] We studied the differential conductance channels of this junction under bias and gate voltages using Landauer's theory,[23] based on the ground-state DFT Hamiltonian. We found that the conductance of this junction is controlled by an interplay of quantum interference, charging, Coulomb blockade, and electron−hole binding energy effects.

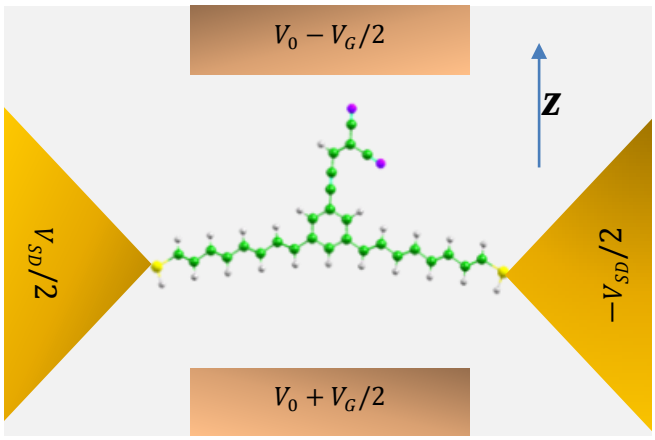

Figure 1: Schematic depiction of the molecular junction in ref. [1]: two thiol- terminated trans-polyacetylene PA segments ($SH-(HC=CH)_4-$) acting as meta substituents on the aromatic ring of a Benzene-molononitrile (MN) molecule. The gate potential V_0, the gate bias V_G and the source drain bias V_{SD} are adjustable. The PAs are electron donors determining the ionization potential of the molecule (I~6.9 eV). The MN is an electron acceptor, endowing the molecule with electron affinity A~1.0 eV. DFT calculations showed that a gate field beyond a critical value of $E_z^* = 0.63$ V/Å inspires spontaneous electron transfer from donor (PA) to acceptor (MN).

In this paper, we continue to study this system focusing on non-equilibrium effects, neglected in Landauer's approach, important because of the large bias voltages used. The most natural choice for this task would be to use a DFT-nonequilibrium Green function methodology,[24] successful in characterizing transport properties of molecular junctions in the off-resonant tunneling regime.[25-31] However, at resonance the approach is less successful, mainly because of the spurious orbital energies of KS-DFT.[22,32] Thus we turn instead to an approach of building a many-body model for the junction and treat transport in terms of many-body states of an isolated molecule. Such a formulation has the advantage of taking into account all the on-the-molecule correlations exactly, and simplifies consideration of resonant tunneling regime when the molecule is weakly coupled to the contacts. Within this

* Emails: roi.baer@huji.ac.il; migalperin@ucsd.edu

approach we mention real-time perturbation theories,[33-36] generalized quantum master equation schemes,[37-41] nonequilibrium pseudoparticles [42-48] and Hubbard Green functions.[15,49-52].

The present paper will also make use of the molecular state-based approach to study conductance switching and identify transport channels in the molecular junction far from equilibrium. For this, we build a model that captures the essential physics of the molecular junction, described in section 0. The conductance of the system, based on this model is studied first at equilibrium (section 0) followed by a non-equilibrium treatment (section III). Of the many approaches developed for studying non-equilibrium conductance (see books and review Refs. [53-56]) we use the Redfield and Lindblad QME formulations,[57-62] which are appropriate when the conductor is weakly coupled to the leads. This level of theory is enough for our demonstration purposes. Further discussion of these theories, their weaknesses and strengths appears in section IIII. We summarize and discuss the main conclusions in section V.

II. HUBBARD MODEL OF THE JUNCTION

Our model assumes that all non-frontier electrons in the molecule are frozen in low-lying orbitals and we need to consider only two frontier orbitals. For this, we employ a double quantum-dot Hubbard model, where the first quantum dot (QD1) represents the LUMO of the acceptor and the second (QD2) the HOMO of the conjugated donor (see Figure 2). This model captures the essential characteristics of the molecule as determined by the DFT calculations. Under zero bias and gate the donor site QD2 is electrically neutral and since it represents the molecular HOMO it holds two active electrons and thus also has a static ("nuclear") charge of $q_2 = 2$. The acceptor site QD1 is also electrically neutral and since it represents the molecular LUMO it holds no active electrons and thus has a static charge of $q_1 = 0$.

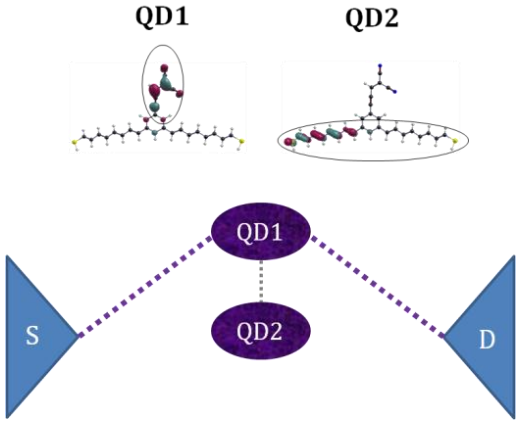

Figure 2: A schematic diagram of the double quantum-dot model, QD1 represents the LUMO (localized on the MN acceptor) and QD2 the HOMO (localized on the PA donor) of the molecule. The two quantum dots couple to each other but only QD1 is directly coupled to the source and drain, because of a destructive interference effect.

The Hubbard Hamiltonian describing the junction is:

$$\hat{H}_{Hub} = \sum_{i=1}^{2} \epsilon_i(E_z)\hat{n}_i + t \sum_{\sigma=\uparrow\downarrow} (\hat{a}_{1\sigma}^{\dagger}\hat{a}_{2\sigma} + cc) + \sum_{i=1}^{2} U_i \hat{n}_{i\uparrow}\hat{n}_{i\downarrow}, \quad (1)$$

where $\hat{a}_{i\sigma}^{\dagger}$ ($\hat{a}_{i\sigma}$) and $\hat{c}_{k\varsigma}^{\dagger}(\hat{c}_{k\varsigma})$ are the electron creation (annihilation) operators for each QD and states in the contacts, respectively. $\hat{n}_{i\sigma} = \hat{a}_{i\sigma}^{\dagger}\hat{a}_{i\sigma}$ is the spin dependent occupations of QD i ($i = 1, 2$ and $\sigma = \uparrow, \downarrow$), and $\hat{n}_i = \hat{n}_{i\uparrow} + \hat{n}_{i\downarrow}$ is the number of electrons on the QD. For future reference we also introduce operator of the total molecular occupation, $\hat{N} = \sum_{i=1}^{2} \hat{n}_i$. The first term in $\hat{H}_{Hubb}$ describes the single particle site energies, where ϵ_i is the orbital energy of an electron in QD i; the second term is the on-site Hubbard repulsion U_i, while the third term couples QD1 to QD2 with the hopping parameter t. The orbital energies are gate-field dependent:

$$\epsilon_i(E_z) = \epsilon_i^0 - e z_i E_z, \quad (2)$$

where E_z is the gate field in direction z and z_i is the vertical position of QD i. ϵ_1^0 is taken as the LUMO energy of the molecule. Since QD2 holds in the molecular ground state 2 electrons ϵ_2^0 is the energy to put the first electron on QD2, i.e. it is the HOMO energy of the molecular *cation*. Then, the on-site repulsion U_2 for the QD2 is determined such that the energy of the second electron in QD2 is the HOMO energy of the neutral molecule:

$$\epsilon^{HOMO} = 2\epsilon_2^0 + U_2. \quad (3)$$

Due to the vertical displacement of the acceptor relative to the donor, the gate field controls the orbital energy difference $\epsilon_1 - \epsilon_2$. It is possible to fix the energy of ϵ_2 so that only ϵ_1 is gate-field dependent (in the model we do this by taking $z_2 = 0$ in Eq. (2)). Achieving this in a laboratory setup (as in Figure 1) requires careful tuning of the metallic potentials.

Table 1: Energetic parameters of the many-body model, Eq. (4).

Parameter	*Value (eV)*	*Explanation*
μ	-5.1	Fermi level of gold
ϵ^{HOMO}	-6.2	From DFT calculation
ϵ^{LUMO}	-1.2	From DFT calculation
ϵ_1^0	-7.8	ϵ^{HOMO} of PA^+ (from DFT calculation)
ϵ_2^0	-1.2	ϵ^{LUMO}
U_1	4.5	$\alpha - \beta$ splitting in DFT calculation after charge transfer
U_2	1.6	$\epsilon^{HOMO} - \epsilon_1^0$
U_{12}	1.8	Exciton binding energy from DFT calculation.
$\Gamma_{1L} = \Gamma_{1R}$	0.005	Assumed electron escape rates
t_{12}	0.001	
q_1	0	See text for explanation.
q_2	2	See text for explanation.

In ref. [1] we found that the long-range attraction between the electron on QD1 and the hole on QD2 formed by intramolecular charge transfer is an important energy scale. To consider this effect, we add to the Hubbard Hamiltonian inter-site

Coulomb interactions terms, forming the molecular junction Hamiltonian:

$$\hat{H}_{\mathrm{M}} = \hat{H}_{Hub}(E_z) + U_{1j}(q_1 - \hat{n}_1)(q_2 - \hat{n}_2) - \mu\hat{N}, \qquad (4)$$

An essential feature of the junction is that the current transport through the molecular LUMO but not through its HOMO. This is due to destructive interference appearing when the PA segments are meta-connected to the benzene ring.[1] In the model this is reflected by coupling only QD1 directly to the contacts, whereas QD2, while coupled to QD1, is not directly coupled to source and drain (see bottom part of Figure 2). The left and right contacts are treated as reservoirs of electrons at adjustable chemical potentials obeying the Fermi-Dirac distribution. The coupling of QD1 to the contact is symmetric and assumes a single coupling parameter $\Gamma_{1L} = \Gamma_{1R}$ (wide band approximation). We give the values of the model parameters in Table 1.

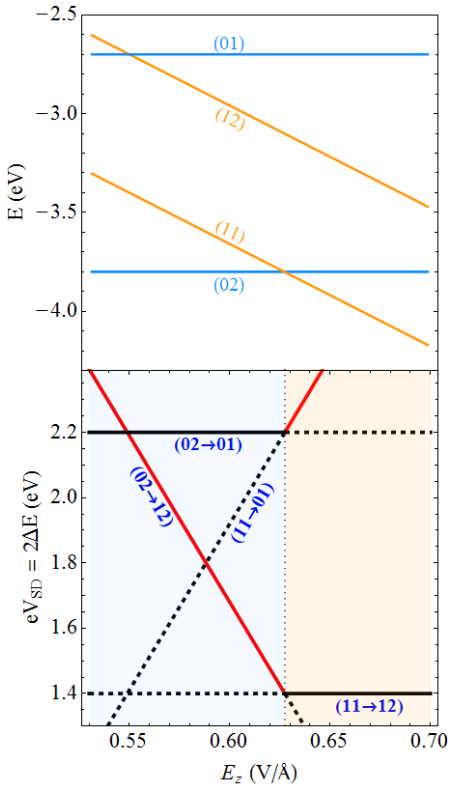

Figure 3: **Top panel:** Low-lying "diabatic" ($t \to 0$) eigenenergies of the model Hamiltonian in Eq. (4) as function of gate field E_z. The states are designated as $(n_1 n_2)$. **Bottom panel:** Selected diabatic energy *differences* (multiplied by 2) from ground state to the nearest hole/electron states as a function of E_z. These can be considered as transition channels in the $V_{SD} - E_z$ plane. The blue (pink) shaded area designates $E_z < E_z^*$ ($E_z > E_z^*$) where (02) ((11)) is the ground state. The red lines are the transition channels that should be active under assumption of equilibrium population distribution. The black doted portion of each line is the regime where this transition channel should not be active due to lack of population of the relevant state. The solid black lines are transition channels that should not be active in the diabatic limit ($t \to 0$) since in this limit QD2 is decoupled from the leads (see text below for details).

We now discuss the energy levels of the Hamiltonian of Eq. (4) assuming $t \to 0$, henceforth called the "diabatic" limit. The state occupations n_1 and n_2 are good quantum numbers and the energies can be labeled as $(n_1\, n_2)$ and some are shown in the top panel of Figure 3 as function of the gate-field E_z. At low gate fields the ground-state is (02) but as E_z grows, the charge-transfer state (11) descends in energy (due to the dependence of ϵ_1 on E_z, see Eq. (2)) and crosses (02) to become the ground-state of the system once $E_z > E_z^*$ where $E_z^* = 0.63\, V/\text{Å}$, is the critical field mentioned in the introduction. Two other low-lying states are plotted, one is the positively charged (01) state, with energy not dependent on E_z (since $n_1 = 0$) and the second is the negatively charged state (12) with energy descending with E_z.

Stating all the relevant energy states we are now in a good starting point to analyze conductance under assumption of equilibrium population in the junction (section III) followed by a non-equilibrium analysis taking into account non-equilibrium effects (section IV).

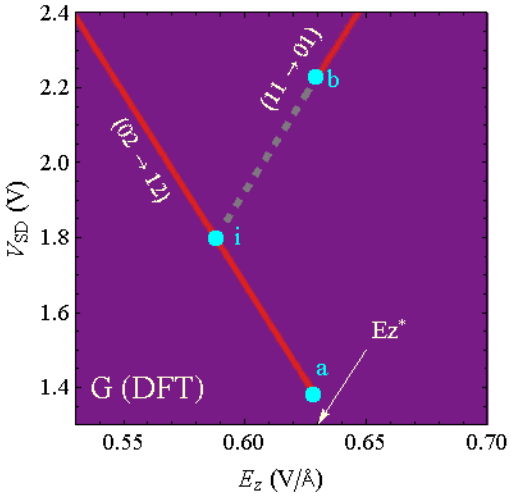

Figure 4: Expected position of the differential conductance peaks as a function of gate field E_z and source-drain bias V_{SD} assuming equilibrium population and $t \to 0$. There are two conducting channels,[63] which can be assigned to the transitions $(02 \to 12)$ and $(11 \to 01)$. At gate fields below E_z^* the active channel $(02 \to 12)$ is electron conducting, while for $E_z > E_z^*$ the active channel $(11 \to 01)$ is hole conducting. The intersection of the red line $(02 \to 12)$ with the extrapolated (dotted) line $(11 \to 01)$ is marked by the point i while points a and b denote, respectively, the ending and the beginning of those channels which occur at the critical gate field E_z^* .

III. CONDUCTANCE UNDER EQUILIBRIUM ASSUMPTION

In equilibrium, the junction is assumed to be in its ground state. The conductance channels are formed by a transition to low-lying states which differ from the ground state by an electron or by a hole. Assuming a symmetric potential drop across the junction, the source-drain potential difference V_{SD} required for causing a transition $(n_1 n_2) \to (n_3 n_4)$ is

$$V_{SD} = 2\Delta E(n_1 n_2 \to n_3 n_4)/e. \qquad (5)$$

In Figure 3 (bottom) we plot the lines (called "transition channels") obeying this relation as a function of the gate field

E_z. At $E_z < E_z^*$, the blue shaded region, the ground state is (02) and the possible transitions are to states (12) requiring energy $2\Delta E(02 \to 12)$ and to (01) requiring $2\Delta E(02 \to 01)$ (see red and black solid lines in the blue shaded region of Figure 3 (bottom)). For $E_z > E_z^*$, the pink shaded region, the ground state becomes (11) and the possible transitions are to state (01) requiring energy $2\Delta E(11 \to 01)$ or to state (12) requiring $2\Delta E(11 \to 12)$ (see red and black solid lines in the pink shaded region of Figure 3 (bottom)). The two remaining transition channels, $(11 \to 21)$ and $(11 \to 10)$ are not considered since they appear at much higher energies.

In the diabatic limit ($t \to 0$), the transport of charge through QD2 is not possible since this dot is decoupled from the leads. Therefore, of the four channels described above, only two, those involving a change in n_1, actually conduct. When $E_z < E_z^*$ the electron conductance channel $(02 \to 12)$ is operative as (02) is the ground state. Similarly, when $E_z > E_z^*$ only $(11 \to 01)$ is active as (11) is the ground state. These considerations allow us to deduce the position of the expected differential conductance peaks as a function of gate field E_z and source-drain bias V_{SD} shown in Figure 4.

IV. NON-EQUILIBRIUM ANALYSIS

The considerations above relied on a simplifying assumption, namely that the bias does not disturb the equilibrium population on the molecule. We now lift this assumption since we use quite large bias voltages and non-equilibrium effects are likely to be important. We employ the Redfield QME, where the weak coupling to the leads is treated as a perturbation. A standard closure procedure allows us to obtain an effective Liouvillian in the molecular subspace. The right eigenvector corresponding to an eigenvalue with zero imaginary part is the steady-state density matrix (SSDM). From the SSDM we compute the steady-state populations, average non-equilibrium current $I(V_{SD})$ and the differential conductance $G = \partial I/\partial V_{SD}$ as a function of V_{SD} for each gate-field.

One well-known shortcoming of Redfield theory is that its SSDM is not guaranteed to be positive definite, as a physical DM should always be. Indeed, in our calculations we do find certain voltage regimes where Redfield QME fails. However, these are not the regimes of interest for this work. Note that we have also used the Lindblad approach[57,58] to compute the conductance and populations and obtained nearly identical results to those of the Redfield theory in the regimes of interest shown below. The Lindblad approach, guarantees positivity of the DM, although it has other basic shortcomings [59]. It is comforting that in the regime of interest both methods gave identical predictions.

We now discuss the results we obtained for the populations P, the steady-state currents I, and the differential conductance peaks G as functions of E_z and V_{SD} (see Figure 5).

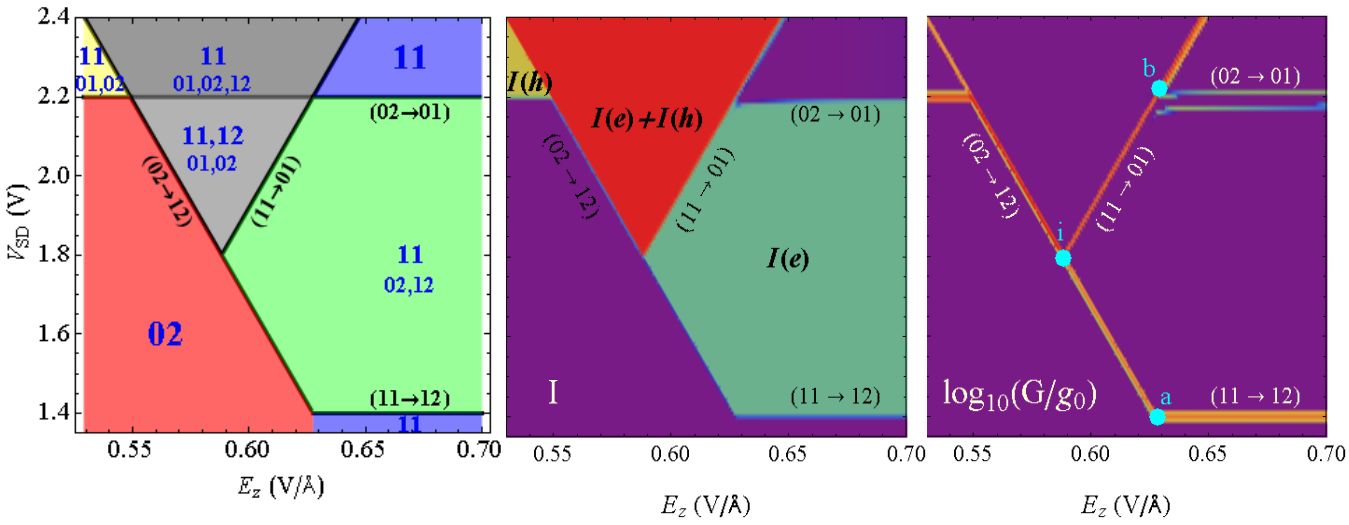

Figure 5: Contour plots of the Redfield prediction for the steady-state distribution of populations $P(02)$, $P(11)$ $P(12)$ and $P(01)$ (left panel), current I (middle panel), and the differential conductance peaks G (right panel) as functions of E_z and V_{SD}. The colors of the different population distribution regimes (left panel) are chosen arbitrarily while the color coding for the current and differential conductance peaks (middle and right panels) have a meaning of intensity (red, orange, yellow, green, blue and purple where red is the highest and purple is zero).

A. Population distribution

The population distribution among the four states, depicted in the left panel of Figure 5, displays a variety of domains, each with its own color and characterized with a different combination of states (in each domain the most populated state appears in large bold letters). This picture is markedly different from the equilibrium population distribution where only two domains, blue and pink, exist (see Figure 3). Furthermore, in equilibrium the line $E_z = E_z^*$ is the boundary while in non-equilibrium the boundaries of the different domains are the transition channels discussed in section 0.

The transition channels form the boundary domains because they designate the threshold conditions for insertion of an electron or a hole into the junction. Such an injected charge carrier brings with it excess energy of $\mu + \frac{eV_{SD}}{2}$ which can be used to populate higher energy states.

It is important to note that the population redistribution

among states with the same number of electrons requires concurrent population change in states of different charge. For example, let us revert Figure 3(top) and consider the transfer of population from (02) to (11) at $E_z = 0.58V/\text{Å}$. The energy for this process is $\Delta E(02 \to 11) = 0.2eV$. Naïvely, one would expect that a source-drain bias of $V_{SD} = 0.4V$ will be the threshold voltage for population of (11). In reality however, the threshold is determined by a totally different process, namely the injection of an electron from the leads, $(02 \to 12)$, which occurs at $\approx 1.9V$. The reason for this odd-looking dependence is simply that at 0K one must rely on injected charge carriers to transfer the available energy in the leads into the junction.

B. Steady-state current

The non-zero steady-state current shown in the middle panel of Figure 5, appears in several distinct domains bounded by the transition channels of the junction:

a) The purple domains designate regimes of zero current.
b) The red triangle defined by the transition channels $(02 \to 12)$ and $(11 \to 01)$ indicates a high current regime which has strong contributions both from electron and hole currents due to the relatively high population of (02) and (11) seen in the left panel.
c) The green colored area on the right is bounded by the four transition channels $(02 \to 01), (11 \to 01), (02 \to 12)$ and $(11 \to 12)$. Dominant contribution to the current comes from the $(02 \to 12)$ electronic transition and it is weak due to the low population of the (02) state. In this regime, the hole conducting channel $(11 \to 01)$ is closed.
d) The yellow triangular region located at the upper left corner is bounded by the transition channels $(02 \to 01)$ and $(02 \to 12)$. The current is solely due to holes passing through the $(11 \to 01)$ conducting channel. The current is intense due to the relatively high population of the (11) state. Interestingly, the current is not due to any of the transitions defining the domain boundaries. These transitions do not contribute, either because they are energetically inaccessible ($(02 \to 12)$) or they change n_2 ($(02 \to 01)$), a process that is weak because QD2 is not directly coupled to the leads.

C. Equilibrium vs. non-equilibrium conductance

The current domains depicted above give rise to sharp differential conductance peaks called "conductance channels" which are displayed in Figure 5 (right). These peaks reveal a richer picture than predicted by the equilibrium theory of Figure 4. In some cases both equilibrium and non-equilibrium conductance channels coincide: for example the electron conducting channel $(02 \to 12)$ and the hole conducting channel $(11 \to 01)$, for $E_z > E_z^*$. But under non-equilibrium conditions additional channels appear. One such case is the hole conducting channel $(11 \to 01)$ when $E_z < E_z^*$ (the segment connecting points i and b in Figure 5 (right)). To activate this channel one should have a significant population of the (11) state. In equilibrium (11) is not populated at all because $E_z < E_z^*$ (blue domain in Figure 3) while in non-equilibrium it carries a significant population (grey domain in Figure 5(left)) for reasons discussed above.

Additional non-equilibrium conductance channels, absent from the equilibrium picture, appear as horizontal lines in Figure 5 (right) at $V_{SD} = 1.4V$ and $V_{SD} = 2.2V$. These are attributed to the transitions $(02 \to 01)$ and $(11 \to 12)$ respectively. Their presence is somewhat surprising since the underlying transitions involve a change in the population of QD2, which is not directly coupled to the leads. Obviously the population of (01) or (12) must involve indirect mechanisms. For example, $02 \to 11 \to 01$ or $11 \to 02 \to 12$ respectively, both involve an internal charge reorganization step. Once the population of QD2 changes, a redistribution of population is enforced on all other states as well (because the sum of all populations is always unity) and this indirectly affects the current in all the current-carrying channels.

V. SUMMARY

We have studied the conductance of the molecular junction depicted in Figure 1, under an external gate field and source-drain bias. This junction was considered in our previous paper where we studied the conductance using a ground-state Hamiltonian, based on a DFT for which the orbital energies are close to the quasiparticle energies and employing Landauer's formula [1] which describes the conductance of non-interacting particles. In this paper, we have focused on interaction-induced non-equilibrium effects, neglected in our previous treatment, which are likely to be important due to the large bias voltages used. Using the data and insights provided by the DFT calculations we built a double quantum-dot Hubbard Hamiltonian to describe this junction. We then employed a non-equilibrium many-body approach based on the Redfield theory to calculate the steady-state populations, current and conductance channels of this junction. We used the same model Hamiltonian to construct the conductance channels of this junction at equilibrium.

We found that in some cases both equilibrium and non-equilibrium conductance channels coincide; for example the electron conducting channel $(02 \to 12)$ and the hole conducting channel $(11 \to 01)$, for $E_z > E_z^*$. But in non-equilibrium additional channels appear, for example $(11 \to 12)$ and $(02 \to 01)$. Another example is the appearance of a "missing segment" in the conductance channel, as $(11 \to 01)$ between points i and b (see Figure 5 (right)). At equilibrium, the line $E_z = E_z^*$ is the boundary separating the regimes of population distribution (Figure 3(bottom)) and thus, determines the activation\deactivation of the conducting channels. At non-equilibrium the boundaries of the different population domains are very different in shape (Figure 5 (left)), determined by the transition channels.

In this system, the non-equilibrium population distribution is the most important factor determining the activation/deactivation of conducting channels. This effect is not related to the strength of the coupling between the two quantum dots. A change in the population of one of the charged

states (induced by changing E_z or V_{SD}) will necessarily invoke a redistribution of populations (and mutual coherences) of other states and thus will affect the current in other channels. It is for this reason that in non-equilibrium the conductance channels are coincident with transition channels, regardless of the ability of this transition by itself to conduct current. As an example, see the explanation above of why the transition $(11 \rightarrow 12)$, not expected to be conducting in the diabatic limit, is coincident with a conductance channel.

One of the attractive features of the junction is the small number of conductance channels and the sharp response to the gate field. This was predicted by the equilibrium theory, finding only two conductance channels (see Figure 4). The non-equilibrium theory predicts that additional conductance channels form, making the picture somewhat more intricate. However, the number of such channels is still very small and the high tunability properties and sharp switching behavior of this junction (Figure 5 (right)) are preserved.

Future research directions are needed to be studied for this junction. First, we have not yet considered the effect of molecular vibrations, which may be important because their tendency to disrupt the destructive interference through the benzene ring.[64] In addition, the intra-junction charge transfer can also be induced by light instead of by the gate field, allowing opto-electronic switching control.

Acknowledgments: RB gratefully thanks the Israel Science Foundation (ISF) and the US-Israel Binational Science Foundation (BSF) for support of this work. MG gratefully thanks the NSF and the BSF for support of this research.

(1) Baratz, A.; Baer, R. Nonmechanical Conductance Switching in a Molecular Tunnel Junction, *J. Phys. Chem. Lett.* **2012**, *3*, 498-502.
(2) Dekker, C. Carbon nanotubes as molecular quantum wires, *Physics Today* **1999**, *52*, 22-28.
(3) Di Ventra, M.; Pantelides, S. T.; Lang, N. D. The benzene molecule as a molecular resonant-tunneling transistor, *Appl. Phys. Lett.* **2000**, *76*, 3448-3450.
(4) Xue, Y. Q.; Datta, S.; Ratner, M. A. Charge transfer and "band lineup" in molecular electronic devices: A chemical and numerical interpretation, *J. Chem. Phys.* **2001**, *115*, 4292-4299.
(5) Park, J.; Pasupathy, A. N.; Goldsmith, J. I.; Chang, C.; Yaish, Y.; Petta, J. R.; Rinkoski, M.; Sethna, J. P.; Abruna, H. D.; McEuen, P. L.*et al.* Coulomb blockade and the Kondo effect in single-atom transistors, *Nature* **2002**, *417*, 722-725.
(6) Liang, W. J.; Shores, M. P.; Bockrath, M.; Long, J. R.; Park, H. Kondo resonance in a single-molecule transistor, *Nature* **2002**, *417*, 725-729.
(7) Zhitenev, N. B.; Meng, H.; Bao, Z. Conductance of small molecular junctions, *Phys. Rev. Lett.* **2002**, *88*, 226801.
(8) Heath, J. R.; Ratner, M. A. Molecular electronics, *Physics Today* **2003**, *56*, 43-49.
(9) Yang, Z. Q.; Lang, N. D.; Di Ventra, M. Effects of geometry and doping on the operation of molecular transistors, *Appl. Phys. Lett.* **2003**, *82*, 1938-1940.
(10) Kubatkin, S.; Danilov, A.; Hjort, M.; Cornil, J.; Bredas, J. L.; Stuhr-Hansen, N.; Hedegard, P.; Bjornholm, T. Single-electron transistor of a single organic molecule with access to several redox states, *Nature* **2003**, *425*, 698-701.
(11) Champagne, A. R.; Pasupathy, A. N.; Ralph, D. C. Mechanically adjustable and electrically gated single-molecule transistors, *Nano Lett.* **2005**, *5*, 305-308.
(12) Kaun, C. C.; Seideman, T. The gating efficiency of single-molecule transistors, *J Comput Theor Nanos* **2006**, *3*, 951-956.
(13) Song, B.; Ryndyk, D. A.; Cuniberti, G. Molecular junctions in the Coulomb blockade regime: Rectification and nesting, *Phys. Rev. B* **2007**, *76*, 045408.
(14) Galperin, M.; Nitzan, A.; Ratner, M. A. Inelastic effects in molecular junctions in the Coulomb and Kondo regimes: Nonequilibrium equation-of-motion approach *Phys. Rev. B* **2007**, *76*, 035301.
(15) Galperin, M.; Nitzan, A.; Ratner, M. A. Inelastic transport in the Coulomb blockade regime within a nonequilibrium atomic limit, *Phys. Rev. B* **2008**, *78*, 125320.
(16) Kocherzhenko, A. A.; Siebbeles, L. D. A.; Grozema, F. C. Chemically Gated Quantum-Interference-Based Molecular Transistor, *J. Phys. Chem. Lett.* **2011**, *2*, 1753-1756.
(17) Park, H.; Park, J.; Lim, A. K. L.; Anderson, E. H.; Alivisatos, A. P.; McEuen, P. L. Nanomechanical oscillations in a single-C-60 transistor, *Nature* **2000**, *407*, 57-60.
(18) Ghosh, A. W.; Rakshit, T.; Datta, S. Gating of a Molecular Transistor: Electrostatic and Conformational, *Nano Lett.* **2004**, *4*, 565-568.
(19) Meded, V.; Bagrets, A.; Fink, K.; Chandrasekar, R.; Ruben, M.; Evers, F.; Bernand-Mantel, A.; Seldenthuis, J. S.; Beukman, A.; van der Zant, H. S. J. Electrical control over the Fe(II) spin crossover in a single molecule: Theory and experiment, *Phys. Rev. B* **2011**, *83*, 245415.
(20) Baer, R.; Livshits, E.; Salzner, U. "Tuned" Range-separated hybrids in density functional theory, *Ann. Rev. Phys. Chem.* **2010**, *61*, 85-109.
(21) Stein, T.; Kronik, L.; Baer, R. Reliable Prediction of Charge Transfer Excitations in Molecular Complexes Using Time-Dependent Density Functional Theory, *J. Am. Chem. Soc.* **2009**, *131*, 2818-2820.
(22) Stein, T.; Eisenberg, H.; Kronik, L.; Baer, R. Fundamental gaps of finite systems from the eigenvalues of a generalized Kohn-Sham method, *Phys. Rev. Lett.* **2010**, *105*, 266802.
(23) Landauer, R. *IBM Journal of Research ond Development* **1957**, *1*, 223.
(24) Xue, Y. Q.; Datta, S.; Ratner, M. A. First-principles based matrix Green's function approach to molecular electronic devices: general formalism, *Chem. Phys.* **2002**, *281*, 151-170.
(25) Brandbyge, M.; Mozos, J. L.; Ordejon, P.; Taylor, J.; Stokbro, K. Density-functional method for nonequilibrium electron transport, *Phys. Rev. B* **2002**, *65*.
(26) Frederiksen, T.; Paulsson, M.; Brandbyge, M.; Jauho, A. P. Inelastic transport theory from first principles: Methodology and application to nanoscale devices, *Phys. Rev. B* **2007**, *75*.
(27) Stefanucci, G.; Almbladh, C.-O.; Kurth, S.; Gross, E. K. U.; Rubio, A.; van Leeuwen, R.; Dahlen, N. E.; von Barth, U. Time-Dependent Transport Through Single Molecules: Nonequilibrium Green's Functions. In *Time-Dependent Density Functional Theory*; Marques, M. A. L., Ullrich, C. A., Nogueira, F., Rubio, A., Burke, K., Gross, E. K. U., Eds.; Springer: Berlin, 2006; Vol. 706; pp 479.
(28) Sergueev, N.; Demkov, A. A.; Guo, H. Inelastic resonant tunneling in C-60 molecular junctions, *Phys. Rev. B* **2007**, *75*.
(29) Schull, G.; Frederiksen, T.; Brandbyge, M.; Berndt, R. Passing Current through Touching Molecules, *Phys. Rev. Lett.* **2009**, *103*.
(30) Avriller, R.; Frederiksen, T. Inelastic shot noise characteristics of nanoscale junctions from first principles, *Phys. Rev. B* **2012**, *86*, 155411.
(31) Kim, Y.; Garcia-Lekue, A.; Sysoiev, D.; Frederiksen, T.; Groth, U.; Scheer, E. Charge Transport in Azobenzene-Based Single-Molecule Junctions, *Phys. Rev. Lett.* **2012**, *109*, 226801.

(32) Galperin, M.; Tretiak, S. Linear optical response of current-carrying molecular junction: A nonequilibrium Green's function-time-dependent density functional theory approach, *J. Chem. Phys.* **2008**, *128*.
(33) Schoeller, H.; Schon, G. Mesoscopic Quantum Transport - Resonant-Tunneling in the Presence of a Strong Coulomb Interaction, *Phys. Rev. B* **1994**, *50*, 18436-18452.
(34) Utsumi, Y.; Martinek, J.; Schon, G.; Imamura, H.; Maekawa, S. Nonequilibrium Kondo effect in a quantum dot coupled to ferromagnetic leads, *Phys. Rev. B* **2005**, *71*, 245116.
(35) Leijnse, M.; Wegewijs, M. R. Kinetic equations for transport through single-molecule transistors, *Phys. Rev. B* **2008**, *78*, 235424.
(36) Koller, S.; Grifoni, M.; Leijnse, M.; Wegewijs, M. R. Density-operator approaches to transport through interacting quantum dots: Simplifications in fourth-order perturbation theory, *Phys. Rev. B* **2010**, *82*.
(37) Ovchinnikov, I. V.; Neuhauser, D. A Liouville equation for systems which exchange particles with reservoirs: Transport through a nanodevice, *J. Chem. Phys.* **2005**, *122*, 024707.
(38) Schaller, G.; Kiesslich, G.; Brandes, T. Transport statistics of interacting double dot systems: Coherent and non-Markovian effects, *Phys. Rev. B* **2009**, *80*, 245107.
(39) Pedersen, J. N.; Wacker, A. Tunneling through nanosystems: Combining broadening with many-particle states, *Phys. Rev. B* **2005**, *72*, 195330.
(40) Esposito, M.; Galperin, M. Transport in molecular states language: Generalized quantum master equation approach, *Phys. Rev. B* **2009**, *79*, 205303.
(41) Esposito, M.; Galperin, M. Self-Consistent Quantum Master Equation Approach to Molecular Transport, *J. Phys. Chem. C* **2010**, *114*, 20362-20369.
(42) Wingreen, N. S.; Meir, Y. Anderson Model out of Equilibrium - Noncrossing-Approximation Approach to Transport through a Quantum-Dot, *Phys. Rev. B* **1994**, *49*, 11040-11052.
(43) Sivan, N.; Wingreen, N. S. Single-impurity Anderson model out of equilibrium, *Phys. Rev. B* **1996**, *54*, 11622-11629.
(44) Hettler, M. H.; Kroha, J.; Hershfield, S. Nonequilibrium dynamics of the Anderson impurity model, *Phys. Rev. B* **1998**, *58*, 5649-5664.
(45) Eckstein, M.; Werner, P. Nonequilibrium dynamical mean-field calculations based on the noncrossing approximation and its generalizations, *Phys. Rev. B* **2010**, *82*, 115115.
(46) Oh, J. H.; Ahn, D.; Bubanja, V. Transport theory of coupled quantum dots based on the auxiliary-operator method, *Phys. Rev. B* **2011**, *83*, 205302.
(47) White, A. J.; Galperin, M. Inelastic transport: a pseudoparticle approach, *Phys. Chem. Chem. Phys.* **2012**, *14*, 13809-13819.
(48) White, A. J.; Fainberg, B. D.; Galperin, M. Collective Plasmon-Molecule Excitations in Nanojunctions: Quantum Consideration, *J. Phys. Chem. Lett.* **2012**, *3*, 2738-2743.
(49) Sandalov, I.; Johansson, B.; Eriksson, O. Theory of strongly correlated electron systems: Hubbard-Anderson models from an exact Hamiltonian, and perturbation theory near the atomic limit within a nonorthogonal basis set, *Int. J. Quant. Chem.* **2003**, *94*, 113-143.
(50) Fransson, J. Nonequilibrium theory for a quantum dot with arbitrary on-site correlation strength coupled to leads, *Phys. Rev. B* **2005**, *72*.
(51) Sandalov, I.; Nazmitdinov, R. G. Shell effects in nonlinear magnetotransport through small quantum dots, *Phys. Rev. B* **2007**, *75*, 075315.
(52) Yeganeh, S.; Ratner, M. A.; Galperin, M.; Nitzan, A. Transport in State Space: Voltage-Dependent Conductance Calculations of Benzene-1,4-dithiol, *Nano Lett.* **2009**, *9*, 1770-1774.
(53) Datta, S. *Electronic Transport in Mesoscopic Systems*; Cambridge University Press: Cambridge, 1995.
(54) Haug, H.; Jauho, A.-P. *Quantum kinetics in transport and optics of semiconductors*, 2nd, substantially rev. ed.; Springer: Berlin ; New York, 2008.
(55) Di Ventra, M. *Electrical transport in nanoscale systems*; Cambridge University Press: Cambridge, 2008.
(56) Nitzan, A. Electron transmission through molecules and molecular interfaces, *Ann. Rev. Phys. Chem.* **2001**, *52*, 681-750.
(57) Lindblad, G. Generators of Quantum Dynamical Semigroups, *Communications in Mathematical Physics* **1976**, *48*, 119-130.
(58) Davies, E. B. *Quantum theory of open systems*; Academic Press: London ; New York, 1976.
(59) Kohen, D.; Marston, C. C.; Tannor, D. J. Phase space approach to theories of quantum dissipation, *J. Chem. Phys.* **1997**, *107*, 5236-5253.
(60) Breuer, H.-P.; Petruccione, F. *The theory of open quantum systems*; Oxford University Press: Oxford ; New York, 2002.
(61) Nitzan, A. *Chemical dynamics in condensed phases : relaxation, transfer and reactions in condensed molecular systems*; Oxford University Press: Oxford ; New York, 2006.
(62) Harbola, U.; Esposito, M.; Mukamel, S. Quantum master equation for electron transport through quantum dots and single molecules, *Phys. Rev. B* **2006**, *74*.
(63) The term conducting channel is a conductance peak as function of the source-drain potential difference and gate field.
(64) Hartle, R.; Butzin, M.; Rubio-Pons, O.; Thoss, M. Quantum Interference and Decoherence in Single-Molecule Junctions: How Vibrations Induce Electrical Current, *Phys. Rev. Lett.* **2011**, *107*, 046802.